State-selective Rydberg excitation with femtosecond pulses

M. Kozák,[1] J. Preclíková,[2] D. Fregenal,[3] and J. P. Hansen[2]

[1]*Faculty of Mathematics and Physics, Charles University in Prague, Ke Karlovu 3, CZ-121 16 Prague 2, Czech Republic*

[2]*Department of Physics and Technology, University of Bergen, N-5007 Bergen, Norway*

[3]*Centro Atómico Bariloche and Consejo Nacional de Investigaciones Cientícas y Técnicas, R8402AGP S.C. de Bariloche, Argentina*

(Received 25 January 2013; published 22 April 2013)

We show that multipulse excitation of Rydberg atoms with a sequence of short time-delayed femtosecond pulses results in strong n selection of the final-state amplitudes. In the experiment, a 150 fs laser pulse, which alone populates n levels from 22–32 in Li, is chopped into four time-delayed excitation pulses, which results in a strong modification of the n-level distribution. The mechanism demonstrated in the experiment is derived theoretically: With more pulses, it is shown that the population of a single or a few n levels can be performed *on demand* and varied as long as the central laser frequency is given.

DOI: 10.1103/PhysRevA.87.043421 PACS number(s): 32.80.Rm, 06.60.Jn, 82.53.Kp

Controlling and addressing internal degrees of freedom in Rydberg atoms plays a crucial role in preparing and manipulating the collective behavior of an ensemble of such atoms. This is specifically true in the context of utilizing Rydberg atoms for quantum information. The Rydberg blockade mechanism [1], for example, requires excitation of a single atom to a linear combination of states which has a dipole moment large enough to prohibit excitation of surrounding atoms in the ground state. In the simplest scheme, the excitation to a single n level requires laser pulses with a narrow bandwidth, which in practice involves nanosecond or cw lasers. An alternative is to apply various control algorithms which by means of a final complicated pulse shape may optimize a fast single n transition [2,3]. However, the physics of the excitation scheme will then be "hidden" and no guarantee exists for reaching the final states with close to unit probability when the initial conditions change slightly.

The exposure of quantum systems to a time-separated double set of interactions, since invented by Norman Ramsey more than 60 years ago [4], has developed into a versatile high-precision measurement principle. Today it encompasses a broad band of techniques, such as the atomic streak camera [5], reconstruction of attosecond beating by inferring two-photon transitions [6], and femtosecond pump-probe techniques [7]. In the latter case, the output of the second interaction is based on coherent time evolution of the quantum system between two interacting pulses with controlled time separation τ. This evolution between the pulse interactions often manifests itself as so-called Ramsey fringes, i.e., oscillations in the excited-state probability $\propto \cos(\omega_{ng}\tau)$, where ω_{ng} is the characteristic frequency of the transition. Realization of Ramsey fringes by double-pulse excitation of Rydberg atoms was proposed about 20 years ago [8] and opened a new subfield, *Rydberg wave-packet interferometry* [9–16]. Recently, a generalization of the two-pulse method to a three-pulse optical excitation scheme which eliminates the light shift of the transition frequency was experimentally verified [17].

In this paper, we extend the double-pulse method in Rydberg interferometry and report an experiment based on four-pulse excitation. We demonstrate that the use of more pulse pairs, with a careful selection of delay times, may produce modulated fringe patterns which can permanently suppress or enhance certain otherwise equally accessible final states of a two-pulse experiment. In the extreme case, it will populate a single selected n level while all others are suppressed. Our multipulse excitation scheme thus opens the way for future time-resolved experiments with a single specified Rydberg level excited on a femtosecond or picosecond time scale.

In the experiment, we use lithium atoms which are excited into the $3d$ state by a sequence of two nanosecond pulses. For excitation of the Rydberg wave packet, we apply amplified 150 fs pulses at wavelength $\omega_l = 834$ nm. The detailed excitation conditions are described in [18]. The scheme of the interferometer for controlling the four-pulse experiment is shown in Fig. 1: The main core is created by the Michelson interferometer with two output beams. Each output contains two delayed femtosecond pulses. Due to the different number of reflections in their trajectories, the first pair has time separation Δt, while the second has $\Delta t + \pi/\omega_l$. An additional delay line enables us to control the short-time delay τ between pulses in a pair. All four pulses were coherently connected at a second beam splitter. In the case of the two-pulse experiment, one of the arms of the core Michelson interferometer is blocked. The final population of n states was determined by the selective field ionization (SFI) technique. The pulse energy, 1 μJ, and the spot size of the excitation beam, 50 μm, lead to the peak intensity, $I = 150$ GW/cm^2.

Examples of SFI spectra from measurements at two different positions of the interferometer translation mirror (which correspond to delay time $\Delta t = 280$ and 510 fs) are shown in the two bottom panels of Fig. 1, while the spectra obtained with the two-pulse experiment is in the second panel. The vertical axis corresponds to the ionization time and the horizontal axis corresponds to the time delay τ [19]. We observe a strong periodic signal at certain ionization times and a much weaker modulation at others. This can be directly translated into preferred population of certain Rydberg n levels at given time delay τ by adding horizontal cuts of the SFI spectra [18]. The signal from the two-pulse experiments, shown in Fig. 1(b), demonstrate populated n levels almost in phase.

A theoretical model which explains the experimental result is now derived. We assume that the interacting electric fields can be written as a general sum of pulses which reach their

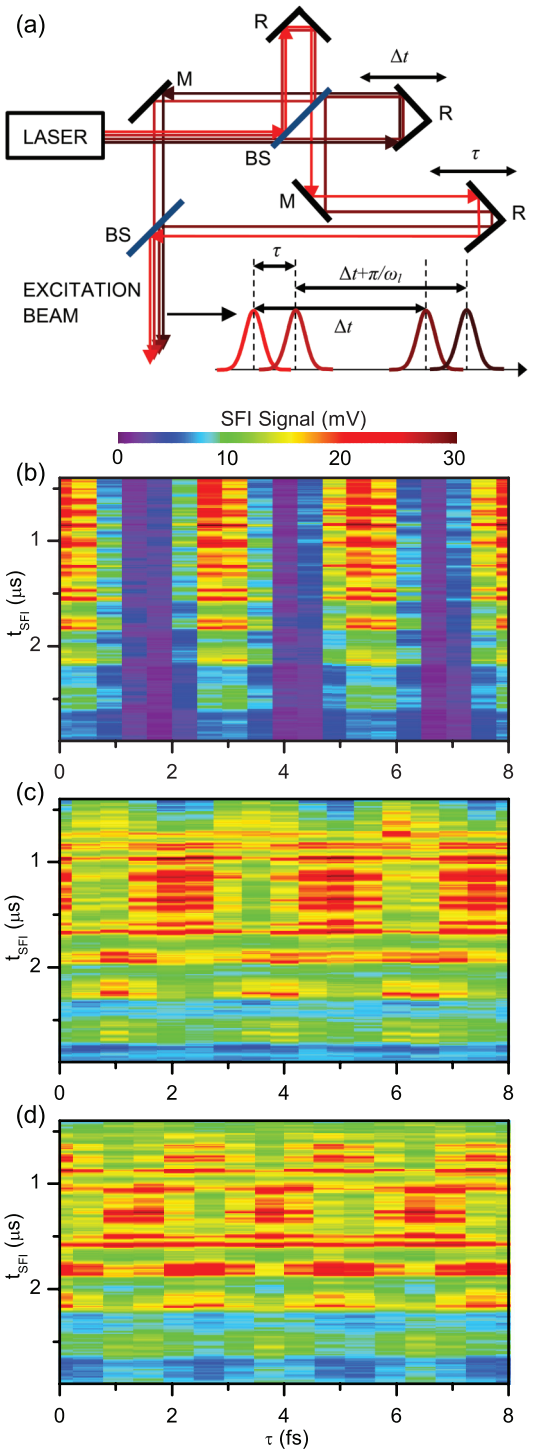

FIG. 1. (Color online) (a) Experimental setup for crossinterferogram measurements with four delayed pulses. M: mirror; R: retroreflector; BS: beam splitter. SFI spectra vs delay time τ, (b) for the case of two pulses and four pulses with pulse-pair time separation (c) $\Delta t = 280$ fs and (d) $\Delta t = 510$ fs.

maximum intensity at delay times τ_i,

$$E(t) = \sum_i E_i g(\alpha_i, t - \tau_i) \sin[\omega_l (t - \tau_i)]. \quad (1)$$

Here, E_i is the maximum electric-field strength of the ith femtosecond pulse, ω_l is the central laser frequency, and the pulse envelope is taken as $g(\alpha,t) = \exp(-\alpha t^2)$. Within first-order perturbation theory, the final-state amplitudes of each Rydberg state n, as a function of delay time τ, can be written as

$$a_n(\tau) = -\tfrac{1}{2}\Omega_n \tilde{E}_0(\Delta_n) \textstyle\sum_i e^{i\omega_{ng}\tau_i}, \quad (2)$$

where Ω_n is the dipole coupling element, $\tilde{E}_0$ is the Fourier transform of the pulse envelope $E_i g(\alpha,t)$, and $\Delta_n = \omega_{ng} - \omega_l$. In the case of two pulses, with pulse delays $\tau_i = \{0,\tau\}$, this expression gives a simple oscillatory expression for the state probabilities P_n as

$$P_n(\tau) = \frac{\tilde{E}_0^2(\Delta_n)\Omega_n^2}{2}[1 + \cos(\omega_{ng}\tau)]. \quad (3)$$

In the four-pulse experiment, the delay times are $\tau_i = \{0,\tau,\Delta t,\Delta t + \tau + \pi/\omega_l\}$. The state probabilities can then be brought to the form

$$P_n(\tau) = \tilde{E}_0^2(\Delta_n)\Omega_n^2[1 + \sin(\omega_{ng}\Delta t)\sin(\omega_{ng}\tau)]. \quad (4)$$

In Fig. 2, we compare the theory of Eqs. (3) and (4) with the main extracted n-level populations of the experiment shown in Figs. 1(b)–1(d). The results display a striking difference between the regular in-phase Ramsey fringes of the two-pulse experiment (upper panel) compared to the four-pulse case (middle, lower panels). In the latter case, some n-level probabilities are strongly enhanced, while others are suppressed or insensitive to the variation in delay time τ. It is also seen that the various n levels are phase modulated with respect to each other and that the phase change depends on the interpair time separation Δt, $\Delta t + \pi/\omega_l$. Overall, the agreement with theory is rather good. The state probabilities which are insensitive to delay time τ correspond to the ones with $\omega_{ng}\Delta t \sim N \times \pi$ for integer N. For noninteger values, the first sine term is responsible for the phase modulation and amplification of the other states. Note, also, that with the present four-pulse setup, no final n states become *dark*, in the sense of being completely unpopulated after the laser interactions for any delay time τ.

However, dark states appear if we change the phase of the last pulse pair and consider the pulse sequence $\tau_i = \{0,\tau,\Delta t,\Delta t + \tau\}$. Experimentally, this can be realized using two independent consecutive Michelson interferometers. In this case, we obtain a different expression for the n-levels probabilities,

$$P_n(\tau) = \tilde{E}_0^2(\Delta_n)\Omega_n^2[1 + \cos(\omega_{ng}\tau)][1 + \cos(\omega_{ng}\Delta t)]. \quad (5)$$

Maximum transfer probability will occur here at delay times $\tau = 2m\pi$ when $\omega_{ng}\Delta t = 2k\pi$ for integer (m,k). The delay time Δt can now be conveniently chosen such that certain final states becomes dark if $\omega_{n'g}\Delta t = (2k+1)\pi$. For example, a central fs laser frequency in resonance with the $3d \rightarrow n = 27$ transition will turn the $n = 28$ level into a dark state with $\Delta t = 1580$ fs. A number of other states will also become strongly suppressed as a result of the last cosine term of Eq. (5). In contrast to the experiment and Eq. (4), all state probabilities will now oscillate with almost identical frequencies ω_{ng}.

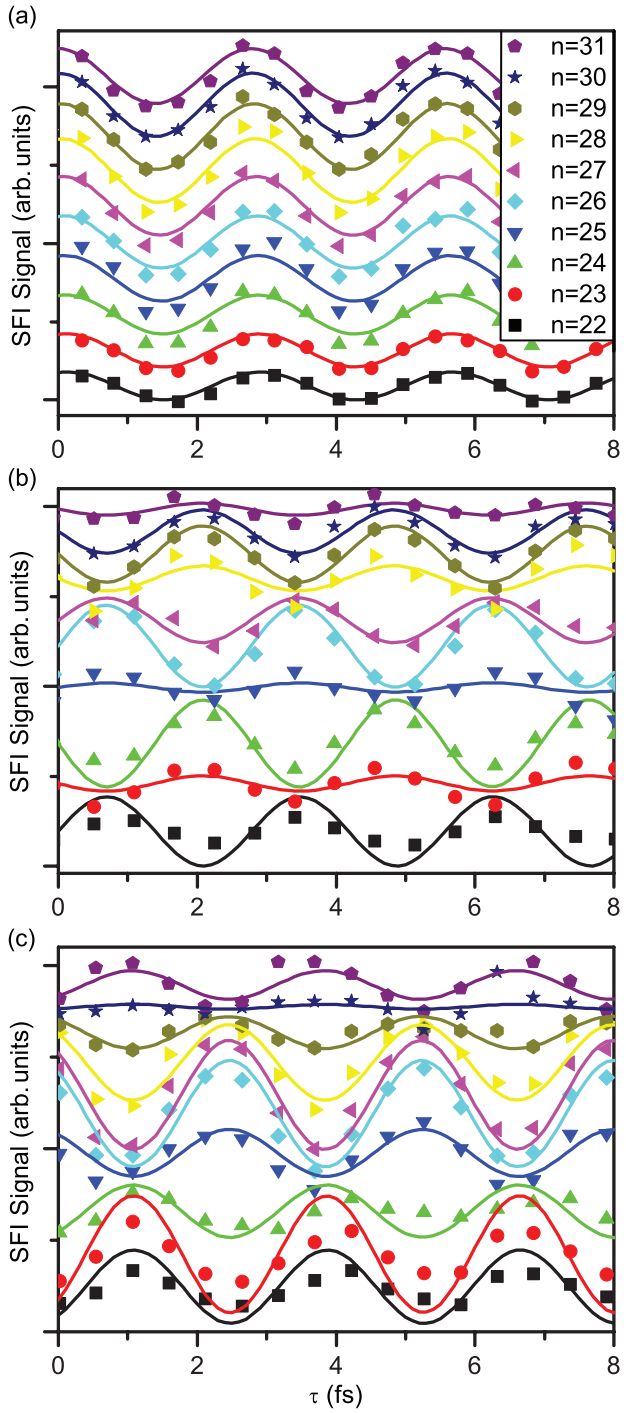

FIG. 2. (Color online) Time evolution of n-level populations (off scale for clarity) extracted from Fig. 1 (points) for (a) two pulses and four pulses with (b) $\Delta t = 280$ fs and (c) $\Delta t = 510$ fs compared with the theory (lines), using (a) Eq. (3) and (b), (c) Eq. (4).

By introducing additional pulse pairs, we can suppress or strengthen any n-state population. For example, by introducing a second delay line resulting in a second time delay Δt_2 between the first and the third pair of pulses, the final expression becomes

$$P_n(\tau) = \tilde{E}_0^2(\Delta_n)\Omega_n^2[1+\cos(\phi_n+\omega_{ng}\tau)] \times[2+\cos(\omega_{ng}\Delta t_1)+\cos(\omega_{ng}\Delta t_2)]. \quad (6)$$

In this expression, we have also introduced a state-dependent phase ϕ_n, which will appear if the second pulse in each pair is chirped with respect to the first [18]. A careful choice of the two delay times $\Delta t_1, \Delta t_2$ and chirp will at certain short delays τ populate a single or two states with most of the total excitation probability.

In order to put the perturbative model on a more solid ground, we solve the time-dependent Schrödinger equation (TDSE) numerically in a basis spanning all relevant final and intermediate states. The basis includes the initial $3d$ state and the p, f states from $n = 10$ to 60. Due to the much smaller d–p dipole couplings as compared to d–f, the population of the p states never exceeds a few percent and can, in fact, be disregarded. The same is true for ionization from the populated f states. The TDSE is then solved numerically for increasing number of pair of pulses given by Eq. (1). In all simulations, we set the laser to be in resonance with the $3d \rightarrow 27f$ transition in lithium.

Figure 3 shows the calculated probabilities as a function of delay τ for the most populated final states. In the upper panel, the Li($3d$) atom is exposed to two pulses, as considered in detail in [18]. As no chirp is applied, all states exhibit the almost same oscillatory dependence on τ on the femtosecond time scale. In the middle panel, an additional pulse pair is added with a delay time chosen such that the $n = 28$ level becomes dark. This results in a strong modification of the remaining populated levels as well. In the lowest panel, we apply four pairs of pulses which are seen to extinguish almost all other n-level populations except the resonant transition. What has been achieved is about 90% population of a single n level with four femtosecond pulse trains. Any n level can reach this fidelity, almost independent of laser intensity and duration, by turning the central laser frequency in resonance with the required transition.

The transient population of the $n = 27$ and the dark final states $n = 26,28$ are shown plotted in Fig. 4 as a function of time. These are the time developments leading to the highlighted final-state probabilities for $\tau = 0$ in Fig. 3. The single-pair simulations display the upbuilding of the final-state probability in all three dominant states (red curves). Similar dynamics, but less pronounced due to weaker individual pulse strength upbuilding, are also seen in the double-pulse case (cyan curves). As the second pulse pair is turned on here at around $t \sim 1000$ fs, the $n = 26,28$ states are seen to decouple (deexcite) and vanish. Similar dynamics is seen in the four-pair case (green curves), but here the resonant $n = 27$ state is gradually building up during each pulse while, as seen in the lower panel of Fig. 3, almost all other states finally vanish.

Finally, it is relevant to compare the present setup, which requires the atoms to be exposed to all time-delayed laser pulses without coherence loss, with the excitation profile of a single pulse with pulse length equal to the largest time delay. In Fig. 5, the n-level distribution for both a weak and a strong single-pulse excitation is compared with the distribution following an eight-pulse sequence. For both long pulses, 5–6 n levels are seen to be important, and the resonant $n = 27$ level contains less than 40% of the total excitation probability. In contrast, in the multipulse scheme, the required $n = 27$ states is seen to contain about 85% of the total excitation

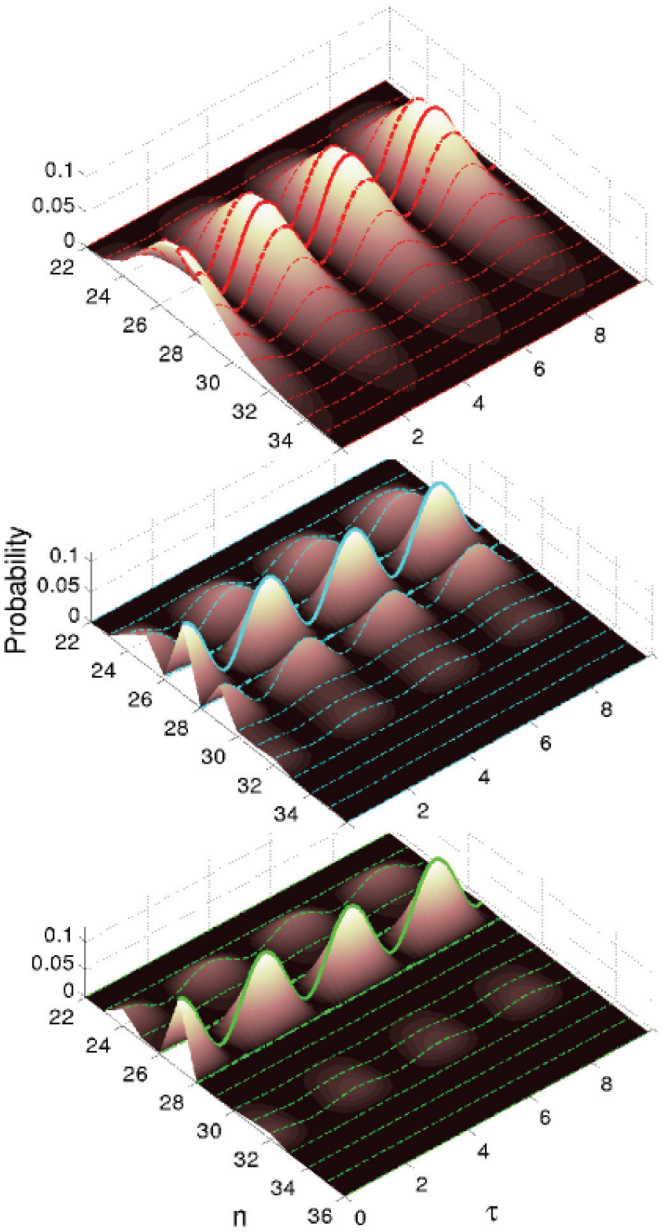

FIG. 3. (Color online) Probabilities for population of the main n levels with a single (upper panel), two (middle panel), and four (lower panel) pairs of fs pulses obtained from a numerical solution of the TDSE. Pulse data: $\Delta t_1 = 1580$ fs, $\Delta t_2 = 789$ fs, $\Delta t_3 = 2369$ fs. The total added pulse energy is the same in all panels.

probability. We are well aware that a clean n selection may be achieved within an equally short excitation time, as our scheme provides, with accessible complex pulse shaper and no limit on the electric-field intensity. Such methods do not, however, offer the same degree of transparency, and require more expensive lasers and control systems. Numerical calculations show that the present results are very stable with respect to laser intensity and pulse lengths of the femtosecond laser. Each individual laser pulse may vary from 10–300 fs and with pulse intensity up to the point that the Rydberg state probabilities reach saturation.

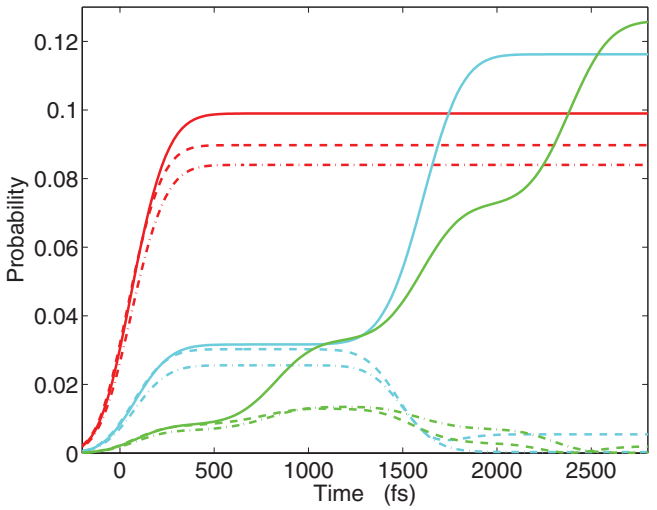

FIG. 4. (Color online) Transient population of the $n = 27$ (full curves), $n = 26$ (broken curves), and $n = 28$ (dash-dotted curves) for $\tau = 0$ of the three simulations of Fig. 3. The red (dark gray) curves are from the single-pulse-pair case (upper panel of Fig. 3); the cyan (light gray) curves are from the double-pulse-pair case (middle panel of Fig. 3), and the green (gray) curves are from the four-pulse-pair case (lower panel of Fig. 3). The first pulse has its maximum at $t = 0$, which implies that the interaction starts at negative t.

In conclusion, we have demonstrated that a sequence of $N > 2$ short-time-separated laser pulses may strongly modify the final Rydberg state population in Li($2d$) $\rightarrow$ Li(nf) excitation. When the time separation between the pulses is carefully chosen, we may selectively populate a single Rydberg level with high fidelity. All other final states well inside the bandwidth of the individual laser pulses will remain dark or very weakly populated. This excitation scheme is likely to be relevant for speedup of gates in quantum information processing with Rydberg atoms. In closing, we

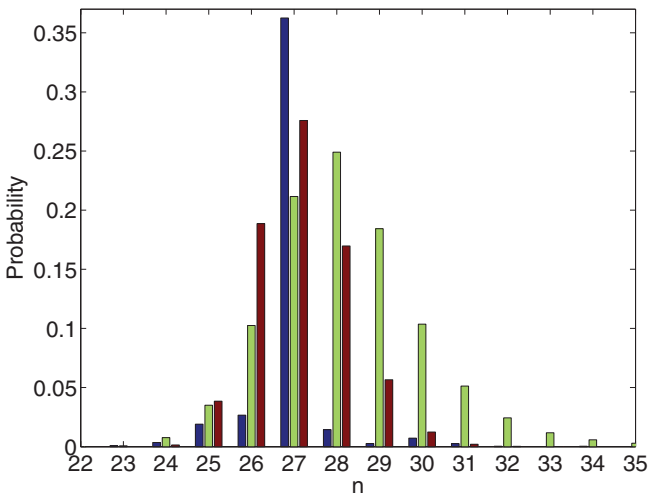

FIG. 5. (Color online) Final-state population of n levels from a eight-pulse sequence (blue bars) compared with a broad ~2000 fs single laser pulse. The brown bars are the results (times 10) from a weak ($E_0 = 10^{-4}$ a.u.) pulse and the green bars are the probabilities from a stronger ($E_0 = 10^{-3}$ a.u.) pulse.

note that time-resolved pulse sequences is an emerging tool within solid-state nanodevices as well [20]. The possibility to selectively populate certain states based on the present setup may well be of importance in that area too.

We thank Ladislav Kocbach for stimulating discussions. This work was supported by the Norwegian Research Council, Czech Science Foundation (Project No. 202/09/H041), and the EU Seventh Framework Programme under Grant Agreement No. PIRSES-GA-2010-269243.

[1] M. D. Lukin, M. Fleischhauer, R. Cote, L. M. Duan, D. Jaksch, J. I. Cirac, and P. Zoller, Phys. Rev. Lett. **87**, 037901 (2001).
[2] J. Ahn, T. C. Weinacht, and P. H. Bucksbaum, Science **287**, 463 (2000).
[3] T. C. Weinacht, J. Ahn, and P. H. Bucksbaum, Nature (London) **397**, 233 (1999).
[4] N. F. Ramsey, Phys. Rev. **76**, 996 (1949).
[5] J. Itatani, F. Quéré, G. L. Yudin, M. Yu. Ivanov, F. Krausz, and P. B. Corkum, Phys. Rev. Lett. **88**, 173903 (2002).
[6] X. He, J. M. Dahlström, R. Rakowski, C. M. Heyl, A. Persson, J. Mauritsson, and A. L'Huillier, Phys. Rev. A **82**, 033410 (2010).
[7] H. Stapelfeldt and T. Seideman, Rev. Mod. Phys. **75**, 543 (2003).
[8] L. D. Noordam, D. I. Duncan, and T. F. Gallagher, Phys. Rev. A **45**, 4734 (1992).
[9] R. R. Jones, C. S. Raman, D. W. Schumacher, and P. H. Bucksbaum, Phys. Rev. Lett. **71**, 2575 (1993).
[10] M. W. Noel, C. R. Stroud, Jr., Phys. Rev. Lett. **75**, 1252 (1995).
[11] D. W. Schumacher, J. H. Hoogenraad, D. Pinkos, and P. H. Bucksbaum, Phys. Rev. A **52**, 4719 (1995).
[12] J. F. Christian and B. Broers, Phys. Rev. A **52**, 3655 (1995).
[13] M. W. Noel and C. R. Stroud, Jr., Phys. Rev. Lett. **77**, 1913 (1996).
[14] X. Chen and J. A. Yeazell, Phys. Rev. A **55**, 3264 (1997).
[15] T. C. Weinacht, J. Ahn, and P. H. Bucksbaum, Phys. Rev. Lett. **80**, 5508 (1998).
[16] R. E. Carley, E. D. Boléat, R. S. Minns, R. Patel, and H. H. Fielding, J. Phys. B **38**, 1907 (2005).
[17] N. Huntemann, B. Lipphardt, M. Okhapkin, Chr. Tamm, E. Peik, A. V. Taichenachev, and V. I. Yudin, Phys. Rev. Lett. **109**, 213002 (2012).
[18] J. Preclíková, M. Kozák, D. Fregenal, Ø. Frette, B. Hamre, B. T. Hjertaker, J. P. Hansen, and L. Kocbach, Phys. Rev. A **86**, 063418 (2012).
[19] Our interferometer was not phase locked, implying that the measurement time is fitted to the absolute (theoretical) time; cf. [18] for a detailed discussion.
[20] J. Lee, T. W. Saucer, A. J. Martin, J. M. Millunchick, and V. Sih, Phys. Rev. Lett. **110**, 013602 (2013).